Taylor & Francis
Taylor & Francis Group

Xenobiotica

the fate of foreign compounds in biological systems

ISSN: 0049-8254 (Print) 1366-5928 (Online) Journal homepage: http://www.tandfonline.com/loi/ixen20

Distribution and metabolism of ^{14}C-Sulfoquinovosylacylpropanediol (^{14}C-SQAP) after a single intravenous administration in tumor-bearing mice

Tatsushi Ruike, Yoshihiro Kanai, Kazuki Iwabata, Yuki Matsumoto, Hiroshi Murata, Masahiro Ishima, Keisuke Ohta, Masahiko Oshige, Shinji Katsura, Koji Kuramochi, Shinji Kamisuki, Hiroeki Sahara, Masahiko Miura, Fumio Sugawara & Kengo Sakaguchi

To cite this article: Tatsushi Ruike, Yoshihiro Kanai, Kazuki Iwabata, Yuki Matsumoto, Hiroshi Murata, Masahiro Ishima, Keisuke Ohta, Masahiko Oshige, Shinji Katsura, Koji Kuramochi, Shinji Kamisuki, Hiroeki Sahara, Masahiko Miura, Fumio Sugawara & Kengo Sakaguchi (2018): Distribution and metabolism of ^{14}C-Sulfoquinovosylacylpropanediol (^{14}C-SQAP) after a single intravenous administration in tumor-bearing mice, Xenobiotica, DOI: 10.1080/00498254.2018.1448949

To link to this article: https://doi.org/10.1080/00498254.2018.1448949

Distribution and metabolism of ^{14}C-Sulfoquinovosylacylpropanediol (^{14}C-SQAP) after a single intravenous administration in tumor-bearing mice

Tatsushi Ruike[1], Yoshihiro Kanai[1], Kazuki Iwabata[1], Yuki Matsumoto[1], Hiroshi Murata[1], Masahiro Ishima[1], Keisuke Ohta[1], Masahiko Oshige[2], Shinji Katsura[2], Koji Kuramochi[1], Shinji Kamisuki[1], Hiroeki Sahara[3], Masahiko Miura[4], Fumio Sugawara[1,*], and Kengo Sakaguchi[1,*]

[1] Department of Applied Biological Science, Faculty of Science and Technology, Tokyo University of Science, 2641 Yamazaki, Noda, Chiba 278-8510, Japan

[2] Department of Environmental Engineering Science, Graduate School of Science and Technology, Gunma University, 1-5-1 Tenjin-cho, Kiryu, Gunma 376-8515, Japan

[3] Laboratory of Biology, Azabu University School of Veterinary Medicine, 1-17-71 Fuchinobe, Chuou-ku, Sagamihara, Kanagawa 252-5201, Japan

[4] Oral Radiation Oncology, Department of Oral Restitution, Graduate School, Tokyo Medical and Dental University, 1-5-45 Yushima, Bunkyo-ku, Tokyo 113-8510, Japan

* Corresponding Authors:

Kengo Sakaguchi: kengo@rs.noda.tus.ac.jp

Fumio Sugawara: sugawara@rs.noda.tus.ac.jp

Department of Applied Biological Science, Faculty of Science and Technology,

Tokyo University of Science,

2641 Yamazaki, Noda, Chiba 278-8510, Japan

ABSTRACT

Sulfoquinovosylacylpropanediol (SQAP) is a novel potent radiosensitizer that inhibits angiogenesis *in vivo* and results in increased hypoxia and reduced tumor volume. We investigated the distribution, metabolism, and excretion of SQAP in male KSN-nude mice transplanted with a human pulmonary carcinoma, Lu65. For the metabolism analysis, a 2 mg (2.98 MBq)/kg of [glucose-U-^{14}C]-SQAP (CP-3839) was intravenously injected. The injected SQAP was decomposed into a stearic acid and a sulfoquinovosylpropanediol (SQP) in the body. The degradation was relatively slow in the carcinoma tissue.1,3-propanediol[1-^{14}C]-SQAP (CP-3635) was administered through intravenous injection of a 1 mg (3.48 MBq)/kg dose followed by whole body autoradiography of the mice. The autoradiography analysis demonstrated that SQAP rapidly distributed throughout the whole body and then quickly decreased within 4 hours except the tumor and excretion organs such as liver, kidney. Retention of SQAP was longer in tumor parts than in other tissues, as indicated by higher levels of radioactivity at 4 hours. The radioactivity around the tumor had also completely disappeared within 72 hours.

Running title: Distribution, metabolism and excretion of ^{14}C-SQAP

Keywords: sulfoquinovosylacylpropanediol (SQAP), ^{14}C-SQAP, radiosensitizer, KSN-nude mice, ADME, human pulmonary carcinoma, tumor xenograft, whole-body autoradiography

INTRODUCTION

There is a need for cancer therapies that cause minimal suffering in cancer patients. One such therapy could be a nontoxic radiosensitizer, which would enable the use of lower doses and provide a wider scope for the irradiation of tumors, including metastatic areas, in patients with terminal disease [Herman et al., 1990; Yuan et al., 2006; Sakaguchi and Sugawara, 2008; Sakaguchi, 2015]. We previously designed and synthesized an agent that we hoped would suit such a purpose. This novel potent radiosensitizer is sulfoquinovosylacylglycerol (SQAG). We subsequently developed a chemically improved successor model, sulfoquinovosylacylpropanediol (SQAP) [Ohta et al., 2001; Aoki et al., 2005; Aoki et al., 2006; Sakimoto et al., 2006; Miura et al., 2007; Sakaguchi and Sugawara, 2008; Takakusagi et al., 2010; Izaguirre-Carbonell et al., 2014; Iwamoto et al., 2015; Sakaguchi, 2015; Sawada et al., 2015; Takakusagi et al., 2015]. By applying the concept of radiosensitization using SQAG or SQAP, a new class of anti-angiogenic treatments has become available. SQAG was originally isolated as a natural product extracted from a red alga, *Gigartina tenella*, and was then chemically synthesized [Hanashima et al., 2000a, 2000b and 2001]. SQAP is a synthetic chemical substance refined from SQAG (see Supplement). Both SQAG and SQAP have great potential for radiosensitization, including the ability to remodel the tumor microenvironment (such as vascular normalization) and reduce adverse effects [Ohta et al., 2001; Sakimoto et al., 2006; Miura et al., 2007; Sakaguchi and Sugawara, 2008; Takakusagi et al., 2010; Sakaguchi, 2015]. To attempt to understand how these compounds affect tumor microenvironments, the whole-body distribution of the successor compound, SQAP, was investigated in mice.

The radiosensitization effect of SQAP is promoted by vascular normalization in the center of a solid tumor under hypoxic conditions (low-oxygen atmosphere), which occurred immediately after administration [Ohta et al., 2001; Takakusagi et al., 2015]. These studies indicated that SQAP could be not only a potent anti-angiogenic agent but also a re-oxidizing agent immediately after administration [Ohta et al., 2001; Takakusagi et al., 2015]. At the radiosensitizing

dose, which differed from the doses of various anti-angiogenic agents developed in the past, SQAP did not cause any remarkable adverse effects and, thus, the limination due to the adverse effects often associated with antitumor therapies [Ohta et al., 2001; Sakimoto et al., 2006; Miura et al., 2007; Sakaguchi and Sugawara, 2008; Takakusagi et al., 2010; Sakaguchi, 2015; Sawada et al., 2015]. To avoid the adverse effects and the limitations caused by anti-angiogenic agents, a new radiotherapy with SQAP used as a radiosensitizer was tested for potential clinical use [Ohta et al., 2001; Takakusagi et al., 2015]. Weak radiation exposure (irradiation) in the presence of low-dose SQAP [Ohta et al., 2001; Takakusagi et al., 2015] was administered to perform the new radiotherapy [Herman et al., Yuan et al., 2006]. However, the optimal combinations of the ionizing radiation and SQAP dose that would provide the most efficient outcomes remained to be determined before SQAP could be clinically implemented.

As shown in Figure 1, SQAP is a novel synthetic derivative of SQAG generated by an organic synthesis that highly sensitizes tumor parts under ionizing radiation [Sakimoto et al., 2006]. The radiosensitization ability of SQAP is the same as that of SQAG [Sakaguchi, 2015]. SQAG is a monoacyl derivative of a sulfolipid (Fig. 1) that has been shown to be an extremely potent radiosensitizer [Hanashima et al., 2000a, 2000b and 2001; Aoki et al., 2005; Ohta et al., 2010; Takakusagi et al., 2011; Izagurrie-Carbonell et al., 2015]. In our laboratory, SQAG was chemically modified to SQAP to eliminate the ambiguous diastereomeric mixture generated from the presence of glycerol in the chemically synthesized SQAG (see Supplement). The diastereomeric mixture is composed of 1-*O*-acyl-3-*O*-(α-D-sulfoquinovosyl) glycerol and 2-*O*-acyl-3-*O*-(α-D-sulfoquinovosyl) glycerol. The mixture occurs via chemical resonance, and separation of the components is very difficult and industrially impossible. This problem made it unlikely that the compound could be officially licensed as a clinical drug. Therefore, we synthesized SQAP by using propanediol without a 2-OH group instead of using glycerol (see Supplement) and confirmed that the biological behavior was the same as that of SQAG [Sakimoto et al., 2006; Ohta et al., 2010; Sawada et al., 2015; Takakusagi et al., 2015].

Sulfolipids are common secondary metabolites that are widely found in photosynthetic bacteria, algae, and higher plants and are mostly food components. Investigations have shown that both SQAG and SQAP have almost no toxic effects following oral administration. This was expected since SQAG is also a component of food plants and SQAP is a derivative. When directly injected *in vivo*, both SQAG and SQAP bound to vascular endothelial growth factor (VEGF) and then reduced the focal adhesion kinase phosphorylation originated from its interaction with VEGF [Izagurrie-Carbonell et al., 2015]. Subsequently, anti-angiogenesis caused by both SQAG and SQAP occurred.

To elucidate the radiosensitization mechanisms of SQAG and SQAP, *in vivo* imaging studies were also conducted to evaluate the SQAP mechanism of action for radiosensitization in tumor parts [Sakimoto et al., 2006; Miura et al., 2007; Sakaguchi and Sugawara, 2008; Takakusagi et al., 2010; Sakaguchi, 2015]. Electron paramagnetic resonance, oxygen imaging revealed that intravenously administered SQAP transiently increased tumor oxygenation in murine SCCVII and human A549 tumor xenografts [Sakimoto et al., 2006; Miura et al., 2007; Sakaguchi and Sugawara, 2008; Takakusagi et al., 2010; Sakaguchi, 2015]. Thus, it was concluded that SQAP transiently increases tumor oxygenation by both pumping O_2 molecules from erythrocytes and improving tumor perfusion, which sensitizes tumors to radiotherapy [Sakimoto et al., 2006; Miura et al., 2007; Sakaguchi and Sugawara, 2008; Takakusagi et al., 2010; Sakaguchi, 2015]. Radiation treatment combined with SQAP significantly delayed angiogenesis-mediated tumor growth and induced remodeling of the tumor microenvironments [Sakimoto et al., 2006; Miura et al., 2007; Sakaguchi and Sugawara, 2008; Takakusagi et al., 2010; Sakaguchi, 2015]. In studies using SQAG, SQAP was found to inhibit angiogenesis *in vivo,* which resulted in increased hypoxia and reduced tumor volume [Sakaguchi, 2015; Sakimoto et al., 2006; Miura et al., 2007; Sakaguchi and Sugawara, 2008; Ohta et al., 2010; Takakusagi et al., 2010].

In the present study, we investigated the absorption, distribution, metabolism, and excretion (ADME) of ^{14}C-labeled SQAP and performed autoradiography in a human Lu65 tumor

xenograft.

MATERIALS AND METHODS

Reagents and Equipment

Scintillator Hionic-Fluor, Scintillator Flo-Scint II and Tissue solubilizer Soluene-350 were obtained from PerkinElmer (Waltham, MA, USA). Saline was obtained from Otsuka Pharmaceutical Factory (Tokushima, Japan). Distilled water for LC/MS and acetonitrile for High-performance liquid chromatography (HPLC) were obtained from Kanto Chemical (Tokyo, Japan). Acetonitrile for LC/MS was obtained from Wako Pure Chemical Industries (Osaka, Japan). Other reagents used in this study were of analytical grade and purchased from Wako Pure Chemical Industries, Nacalai Tesque (Kyoto, Japan), Kanto Chemical or Sigma-Aldrich (St. Louis, MO, USA).

Liquid scintillation counters (LSC) (2500TR, 2700TR, 3100TR or 1900CA, PerkinElmer, MA, USA) were used for the measurement of radioactivity. HPLC system composed of System controller (SCL-10Avp, Shimadzu, Kyoto, Japan), Pump (LC-20AD and LC-10ADvp, Shimadzu), UV detection (SPD-20A and SPD-10Avp, Shimadzu, Kyoto, Japan), Autoinjector (SIL-10ADvp, Shimadzu, Kyoto, Japan), Column oven (CTO-20AC and CTO-10ASvp, Shimadzu, Kyoto, Japan), Online degasser (DGU-20A3 and DGU-14A, Shimadzu, Kyoto, Japan), Manual injector (Rheodyne Model 7725i, Shimadzu, Kyoto, Japan) and Radioactive detector (RAD) (525TR or 625TR, PerkinElmer). LC/MS/MS system composed of MS (LTQ Orbitrap XL, Thermo Fisher Scientific, CA, USA), Pump (LC-10ADvp, Shimadzu, Kyoto, Japan), Autosampler (SIL-HTC, Shimadzu), Column oven (CTO-10ASvp, Shimadzu, Kyoto, Japan), Online degasser (DGU-14A, Shimadzu, Kyoto, Japan) and Radiomatic flow scintillation analyzer (525TR, Packard BioScience, CT, USA). Eighteen of the Lu65 transplanted mice were used for each experiment.

Synthesis of SQAP

Compound 1-*O*-stearoyl-3-*O*-(α-D-sulfoquinovosyl)-1,3-propanediol (SQAP, C18:0; Fig. 1A; R=H) was prepared by organic synthesis as described in the Supplement. The lot number of non-radioactive SQAP was CG-0321 (Lot No. CG-0321).

For autoradiography, radioactive SQAP was prepared from a sulfoquinovose composed of 1,3-propanediol[1-^{14}C] (Fig. 1B). 1,3-propanediol[1-^{14}C]-SQAP (C18:0) was synthesized from 3-benzyloxy-1,3-propanediol[1-^{14}C] in the Korea RadioChemicals Center (KRCC), Gyeonggi Bio-Center, 12FL (864-1, Iui-dong, Yeongtong-gu, Suwon, Korea), by way of Sekisui Medical Co. Ltd., Gyeonggi-do 443-270, Korea) (see Supplement). The chemically synthetic pathway described in our Supplement section was followed by the synthetic method for non-radioactive SQAP [Hanashima et. al., 2000a, 2000b and 2001]. The specific radioactivity of the 1,3-propanediol[1-^{14}C]-SQAP (C18:0) (Lot No. CP-3635) was 3.48 MBq/mg, and the radiochemical purity was 97.5%. The synthetic quantity was 165 MBq.

For the pharmacokinetics study, [glucose-U-^{14}C]-SQAP (C18:0) (Fig. 1C) was prepared by using [glucose-U-^{14}C] as a starting material followed by the synthetic method of non-radioactive SQAP in KRCC [Hanashima et. al., 2000a, 2000b and 2001]. The specific radioactivity of the [glucose-U-^{14}C]-SQAP (C18:0) (Lot No. CP-3839) was 1.49 MBq/mg for the metabolic analysis. The synthetic quantity was 137 MBq.

^{14}C-SQAP expresses ^{14}C-labeled SQAP, including both the 1,3-propanediol[1-^{14}C]-SQAP (Lot No. CP-3635) and the [glucose-U-^{14}C]-SQAP (Lot No. CP-3839). In this paper, 1,3-propanediol[1-^{14}C]-SQAP (CP-3635) denotes the 1,3-propanediol[1-^{14}C]-SQAP (C18:0) (Lot No. CP-3635), and [glucose-U-^{14}C]-SQAP (CP-3839) denotes the [glucose-U-^{14}C]-SQAP (C18:0) (Lot No. CP-3839).

Figure 1A-C indicates the structures of chemically synthesized SQAG, SQAP, and ^{14}C-SQAP. The radiochemical purity was 96.4% 5 days before administration of [glucose-U-^{14}C]-SQAP (CP-3839), and the HPLC column recovery of radioactivity was 98.0%.

The radiochemical purity 1 day after administration (August 3, 2011) was 97.1%, and the HPLC column recovery of radioactivity was 97.5%. ^{14}C-SQAP was administrated intravenously and its dose level of ^{14}C-SQAP was adjusted to around 3 MBq/kg for all the radioisotope experiments.^{14}C-SQAP has undergone Good Laboratory Practice (GLP) compliance inspection, and the GLP-compliant agent is now in a clinical trial for dogs diagnosed with terminal cancer.

Animals

All experimental protocols were approved by the local Laboratory Animal Care and Use Committee of Tokyo University of Science and Tokyo Medical and Dental University. All experiments were carried out in accordance with ADME guidelines. Collected samples were urine, faeces, expired air, carcasses, and cage washes. In addition, collected organs were adrenal gland, bile in gall bladder, blood, bone marrow, brain, brown fat, epididymis, eyeball, fat, gastric contents, harderian gland, heart, intestinal contents, intestine, kidney, liver, lung, mandibular gland, pancreas, pituitary gland, preputial gland, skeletal muscle, skin, spleen, stomach, testis, thyroid gland, tumor, urinary bladder, and urine in bladder.

For the metabolism analysis, a 2 mg (2.98 MBq)/kg of [glucose-U-^{14}C]-SQAP (CP-3839) was intravenously injected to eighteen of mice were used for the experiments of plasma and tumor (3 mice/group, groups were 5 min, 1 h, 2 h, 4h, 8h and 24 h after [glucose-U-^{14}C]-SQAP (CP-3839) administration.).

1,3-propanediol[1-^{14}C]-SQAP (CP-3635) was administered through intravenous injection of a 1 mg (3.48 MBq)/kg dose followed by whole body autoradiography of the mice. Sixteen mice in eight groups of two mice/dose group were given. After 5 min, 1 h, 2 h, 4 h, 8 h, 24 h, 72 h, or 168 h elapsed from the time of the injection.

Six to eight weeks old male KSN nude mice (BALB/cAJcl-nu) were obtained from Sankyo Labo Service Corporation, Inc. (Tokyo, Japan). Tumor transplanting facility was Oral Radiation Oncology, Department of Oral Restitution in Tokyo Medical and Dental University. The mice were transplanted with tumor Lu65, a human cell line with giant cell carcinoma of lung

(JCRB0079). The Lu65 cells were provided by the Japanese Cancer Research Resources Bank. The cells were maintained in RPMI 1640 containing 1 mmol/L pyruvate, 100 units/mL penicillin, and 100 μg/mL streptomycin, supplemented with 10% fetal bovine serum. Bovine aortic endothelial cells were maintained in Eagle's MEM supplemented with 5% fetal bovine serum. The cell lines were maintained at 37^{O}C in a humidified atmosphere containing 5% CO_2.

Lu65 cells, which indicated a high radiation sensitizing effect by applying SQAP to tumor-bearing mice [Sakimoto et al., 2006; Miura et al., 2007; Sakaguchi and Sugawara, 2008; Takakusagi et al., 2010; Sakaguchi 2015], cultured at the Oral Radiation Oncology, Department of Oral Restitution, graduate school of Tokyo Medical and Dental University, were transplanted subcutaneously into male KSN nude mice (tumor xenograft) (2×10^6/animal). After the tumor volume reached 100 to 300 mm^3, or 750 to 1521 mm^3, and the tumor growth was monitored by palpation. The sizes of the palpable tumors were measured by using calipers every 2 days. The tumor volume (V, mm^3) was estimated on the basis of the length (mm) × width (mm) × height (mm) × $\pi/6$. Lu65 is a human giant cell carcinoma of the lung cell line (JCRB0079; Japan Human Sciences Foundation).

Quality Control of Dosing Formulation for Metabolic Analysis

The specific radioactivity of the test substance in the dosing formulation was determined from the ^{14}C-SQAP used at the preparation of the dosing formulation and the collected dosing formulation volume. Just after preparation of the dosing formulation, each aliquot was randomly collected (n = 3) from the dosing formulation. The specific radioactivity of the test substance in the dosing formulation (actual value) was determined from the observed radioactivity concentration in each sample, collected amount of the test substance, and total volume of the dosing formulation to verify within the theoretical value ± 10% (observed value: 103%). ^{14}C-SQAP was administrated intravenously and its dose level of ^{14}C-SQAP was adjusted to around 3 MBq/kg for all the radioisotope experiments.

HPLC Analytical Conditions

The sample was analyzed by HPLC system, and the radioactivity was expressed with RAD that is unit of a physical dose quantity representing the mean energy imported to matter per unit mass by ionizing radiation. An absorbed dose of 1 RAD means that 1 g of material absorbed 100 ergs of energy as a result of exposure to radiation.

Column: CAPCELL PAK C18 MGII, 3 μm, 3.0 mm (I.D.) × 50 mm (L) (Shiseido, Tokyo, Japan)

Mobile phase: A: Acetonitrile

B: 10 mmol/L Ammonium acetate solution

Gradient: Time (min)/B (%) = 0/50 → 20/30 (Linear gradient)

Flow rate: 1 mL/min

Column temperature: 40°C

Run time: 20 min

Injection volume: 8 μL

Sample Collection and Preparation Method

Blood was collected from the inferior vena cava of the mouse using a syringe equipped with a heparin-treated 25-G injection needle and mixed by inversion. The collected blood was immediately centrifuged (8000×g) for 5 min at 4°C to separate plasma and blood cells. A 100 μL aliquot of the plasma was placed in a scintillation vial.

All tumor parts were minced with scissors, placed in a container, and weighed. The minced tumor parts were mixed with 1 mL of saline, weighed, and homogenized using a glass homogenizer. The homogenates (0.5 mL) were placed in a scintillation vial for radioactivity measurement, weighed, and solubilized in 2 mL of Soluene-350 tissue solubilizer, under heating (50−60°C) as described the manufacturer instruction.

Determination of Radioactivity

The radioactivity was measured using LSC after the addition of 10 mL of a Hionic-Fluor scintillator to each sample prepared to determine the radioactivity. The remaining plasma and the tumor homogenates were immediately frozen and stored in a −80ºC deep freezer until use as samples for analysis of radioactivity in plasma and tumors.

Sample Processing

Each sample (plasma: 100 µL, tumor: 0.5 mL) was added to a 3-fold volume of methanol, shaken (10 min), centrifuged (1800×g) for 10 min at 4°C, and then the supernatant was collected. The residue was dissolved in the same volume of methanol as that of the sample preparation, shaken, centrifuged, and then the supernatant was collected. These extraction procedures were performed twice.

The combined supernatants from the experiments performed twice were mixed and made up to the appropriate volume, and an aliquot of the solution was mixed with 10 mL of Hionic-Fluor scintillator to determine the radioactivity. The rest of the residue was dissolved in 2 mL of Soluene-350 tissue solubilizer, made up to appropriate volume, and an aliquot of the solution was mixed with 10 mL of Hionic-Fluor scintillator to determine the radioactivity. The rest of the supernatant was evaporated to dryness and dissolved in HPLC mobile phase, centrifuged (1800×g) for 5 min at 4°C, and the supernatant was analyzed by HPLC. From the counts of radioactivity, the recovery through the sample processing was determined. After the condition was confirmed, column recovery was determined from the samples by HPLC analysis.

Column recovery (%) = [Radioactivity recovered from HPLC in the run time (dpm) / Radioactivity injected to HPLC (dpm)] × 100.

LC/MS (MS^n) Measurement Condition

Analysis sample: Tumor (1 hour after administration, one sample), plasma (1 hour after administration, one sample)

Column: Devolosil C30-UG-5, 4.6 mm I.D. × 250 mm L

Mobile phase: A: 10 mmol/L ammonium acetate

B: Acetonitrile

Gradient: Time (min)/B (%) = 0/0 → 45/90 → 65/90

Ionization: ESI (positive and negative mode)

The reference standards and each of the biological samples were measured by LC/MS (MS^n) to identify and estimate the metabolites under the conditions above. For the analysis, the HPLC eluate was divided by a T-union; approximately 1/5 of the eluate was introduced into the MS, and approximately 4/5 of the eluate was introduced into the Radiomatic flow scintillation analyzer.

The radioactivity in each sample was counted for 2 min by using LSC. The counting efficiency was corrected by the external standard source method. The detection limit of radioactivity was defined as twice the background value and subtracted from the measured radioactivity. The radioactivity in each eluate from HPLC was measured using Radiomatic flow scintillation analyzer. Flo-Scint II scintillator was delivered to the HPLC eluate at a flow rate 3-fold to that of the mobile phase, and the radioactivity (cpm) was integrated by using Radiomatic flow scintillation analyzer at 6-sec intervals. The detection limit of radioactivity was defined as two times the background value and subtracted from the counted radioactivity.

Background Radioactivity of LSC and Radiomatic flow scintillation analyzer

LSC: For the radioactivity assay in the dosing formulation, the solvent used for dilution was analyzed. The column recovery of the HPLC system was analyzed with Radiomatic flow scintillation analyzer. For the radioactivity assay in the biological samples, the plasma was analyzed.

One aliquot of each sample was analyzed.

For the radioactivity assay of the extract, HPLC assay samples and HPLC eluate, extraction solvent, reconstitution solvent, and mobile phase were analyzed to determine the background radioactivity, respectively. For the radioactivity assay in the biological samples, the purified water was analyzed to determine the background radioactivity. The solvent for the dissolution of the reference standard (dissolved in distilled water, and the reference standard (dissolved in 50% ethanol) were analyzed by HPLC, and the mean value of the counts was used as the background radioactivity level.

Radiochemical Purity and Column Recovery

Radiochemical purity (%) was calculated according to the equation shown below from the radioactivity counts in each sample by using a calculation system built in Radiomatic flow scintillation analyzer (Flo-One for Windows Analysis [ver. 3.65], PerkinElmer, MA, USA). Column recovery (%) was calculated according to the equation shown below. The radiochemical purity and column recovery (n = 1 each) were rounded off at the second decimal place and expressed to one decimal place.

Radiochemical purity (%) = (S / T) × 100

T: Total counts over run time (dpm)

S: Counts of peak corresponding to ^{14}C-SQAP (dpm)

The calculating formula of column recovery (%) was shown in Sample Processing.

Dosing Formulation

Specific radioactivity (observed value) of the test substance in the dosing formulation was determined from the radioactivity counts in the dosing formulations by using a data processing system based on the equation shown below according to the following equation:

Observed specific radioactivity (MBq/mg) = A × (T / L)

A: Observed radioactivity concentration (MBq/g)

T: Total volume of dosing formulation (g)

L: Amount of the labeled test substance (mg) of ^{14}C-SQAP

Radioactivity Concentration

Radioactivity concentrations in plasma and tumor were calculated from the radioactivity counts by using a data processing system according to the equation shown below. The radioactivity concentration was converted as ^{14}C-SQAP (ng eq. of ^{14}C-SQAP/g or mL), rounded off to one decimal place, and expressed as an integer. The mean value and the standard deviation (SD) were calculated.

Radioactivity concentration (ng eq./g or mL) = (D / F) × S

D: Radioactivity in assay sample (dpm)

F: Specific radioactivity in dosing formulation (dpm/ng)

S: Amount of sample (g or mL) of ^{14}C-SQAP

Percentage Distribution

The percentage distribution was calculated from the radioactivity counts in tumors by using a data processing system according to the equation shown below. The percentage distribution was converted to a rate for each dosing radioactivity (% of dose), rounded off to the third decimal place, and expressed to two decimal places as the mean value ± SD of three animals.

Percentage distribution (%) = [(D × T) / (A × S)] × 100

D: Radioactivity in assay sample (dpm)

T: Total weight of assay sample (g)

S: Amount of sample (g) ^{14}C-SQAP

A: Administered radioactivity (dpm) which was determined with the specific radioactibity

Analysis of Metabolism

Eighteen of mice were used for the experiments of plasma and tumor (3 mice/group, groups were 5 min, 1 h, 2 h, 4h, 8h and 24 h after [glucose-U-^{14}C]-SQAP (CP-3839) administration.).

1) The recovery through sample processing was rounded off to one decimal place.
2) The radiochromatogram at each analysis was included in this report.
3) The MS radiochromatogram, MS spectrum, and MS^n spectrum at the measurement of LC/MS (MS^n) were included in this report.
4) For the quantitative data of the parent compound and metabolites, the ratio of the countable value of the parent compound to all of the radioactivity detected by HPLC-Radiomatic flow scintillation analyzer analysis was calculated (% on HPLC) and expressed as a ratio for each sample (% in sample) to one decimal place. Moreover, the radioactivity concentrations of the parent compound and metabolites in plasma and tumor were converted to SQAP (ng eq. of SQAP/g or mL), rounded off to one decimal place, and expressed as an integer.

Calculation of Pharmacokinetic (PK) Parameters

Eighteen of mice were used for the experiments of plasma and tumor (3 mice/group, groups were 5 min, 1 h, 2 h, 4h, 8h and 24 h after [glucose-U-^{14}C]-SQAP (CP-3839) administration.). The profiles of radioactivity concentrations in the plasma and tumor were analyzed by non-compartmental analysis in Phoenix WinNonlin Ver. 6.1 (Pharsight), and the following PK parameters were calculated. Data of PK parameters were calculated from the mean concentrations of three animals. For the initial value of $AUC_{t-\infty}$, the observed value was used, and AUC_{0-t} was determined by using the trapezoidal rule.

AUC was rounded up in three digit of significant figure and $t_{1/2}$ was rounded up in two digit of significant figure.

1) AUC were determined form radioactivity concentration-time curve (AUC_{0-t} and $AUC_{0-\infty}$), 1-24 h for Plasma and 4-24 h for Tumor and rounded up in three digit of significant figure
2) Area under the radioactivity concentration-time curve (AUC_{0-t} and $AUC_{0-\infty}$), 1-24 h for Plasma and 4-24 h for Tumor

Statistical Analysis

Statistical comparisons of mean values were performed by using one-way ANOVA. Differences with $P<0.05$ were considered to be statistically significant. Radioactivity concentrations were detected as shown in the Table 2, and conditions were described in HPLC analytical conditions in Material and Methods.

Whole-body Autoradiographic Methods

To analyze whole-body autoradiographic patterns, 1 mg/kg SQAP with the radioactivity (containing 3.48 MBq/mg of 1,3-propanediol[1-^{14}C]-SQAP) was intravenously injected to the tumor-bearing mouse at a time of 5 ml/kg in each of the SQAP group. The same amount of saline was injected for the control group.

Sixteen male KSN nude mice in eight groups of 2 mice/dose group (under GLP conditions) were given. After 5 min, 1 h, 2 h, 4 h, 8 h, 24 h, 72 h, or 168 h elapsed from the time of the injection, the autoradiographies of the mice were captured as follows. Mice were euthanized by CO_2 inhalation. The hair of mice was shaved and the nasal cavity and anus were blocked with 4% carboxymethylcellulose (CMC-Na) and the carcasses were immediately frozen into dried ice and acetone. The frozen blocks were sectioned by using a Leica CM 3600 cryomicrotome maintained at −18℃. Each group was composed of 2 mice. Then, the animals were sacrificed and evaluated by whole-body autoradiography.

Sections were collected at four to six levels of interest and dried in the cryomicrotome chamber. The sections for each mouse were collected on adhesive tape (No. 810, Sumitomo 3M, Japan) at 30-μm thicknesses and then lyophilized. The lyophilized sections were mounted, wrapped with Mitsubishi polyester foil (4 μm, Diafoil; Mitsubishi Plastics), and exposed on high sensitive BAS Storage Phosphor Screens (GE healthcare Life Sciences, NJ, USA) for 24 hours, which was sufficient for the exposure. The exposure screens were scanned by FujiFilm Photo Scanner BAS-2500 (FujiFilm, Tokyo, Japan), and the ionization radiation dose of the screen is expressed with photo-stimulated luminescence (PSL) per unit area as an arbitrary unit.

RESULTS AND DISCUSSION

Determination of Radioactivity Concentration in Tissues for Metabolism

Initially, [glucose-U-^{14}C]-SQAP (CP-3839) was intravenously administered into human adenocarcinoma Lu65 transplanted male KSN nude mice (dose: 2 mg (2.98 MBq)/kg as SQAP). The results are shown in Table 1.

After a single intravenous administration of [glucose-U-^{14}C]-SQAP (CP-3839) to tumor-bearing male mice, the radioactivity concentration in the plasma was 2,229 ng eq./mL at 5 min after administration and decreased time-dependently. The $t_{1/2}$ was 3.1 h (1 to 24 h) (Table 1). The $AUC_{0\text{-}24\,h}$ (area under the concentration-time curve 0 to 24 hours) was 4,400 ng eq.·h/mL and $AUC_{0\text{-}\infty}$ was 4,420 ng eq.·h/mL. The radioactivity concentration in the tumor was 331 ng eq./g 5 min after administration, maintained a comparable level (307–373 ng eq./g) ≤4 h after administration, and then decreased, with a $t_{1/2}$ of 10 h (4–24 h). The $AUC_{0\text{-}24}$ was 4,630 ng eq.·h/g and $AUC_{0\text{-}\infty}$ was 5,730 ng eq.·h/g (Table 1). After 8 h or later of the administration, the radio activity in the tumor is significantly larger than that of the plasma (Table 1).

From these results, soon after a single administration of [glucose-U-^{14}C]-SQAP (CP-3839), the parent compound and/or its metabolites were distributed into the tumor rapidly, and the radioactivity was maintained at a comparable level between the plasma and the tumor until 4 h after administration (Table 1). Thereafter, the radioactivity concentration was higher in the tumor than in the plasma and decreased more slowly than that in the plasma. The $t_{1/2}$ of radioactivity in the tumor was three times as long as that in plasma. However, it was unknown whether the radioactivity levels were related to [glucose-U-^{14}C]-SQAP (CP-3839) or to its metabolites. Therefore, we subsequently performed HPLC radiochromatography of the product.

Analysis of Radioactivity in Plasma and Tumor

After a single intravenous administration of [glucose-U-^{14}C]-SQAP (CP-3839) at a dose of 2 mg/kg, the plasma and tumors obtained from tumor-bearing male mice were analyzed by

HPLC. The radioactivities of the plasma and tumor homogenates were analyzed by HPLC-Radiomatic flow scintillation analyzer, and the ratios of the parent compound and metabolites in each sample were determined.

The recovery levels of radioactivity after sample processing and from the HPLC column after HPLC analysis are shown in Table 2 and indicate that each fraction of SQAP was almost completely recovered. A representative HPLC radiochromatogram of [glucose-U-^{14}C]-SQAP (CP-3839) clearly shows a mono-peak (Fig. 2A). In the plasma (Fig. 2B) and tumor (Fig. 2C), radioactive peaks were detected in HPLC radiochromatograms from 5 minutes to 24 hours after the SQAP administration, and the peaks tended to split into SQAP and another group peak population named Peak 1 (Fig. 2 and Table 3). After 8 h in plasma and after 24 h in tumor, SQAP and Peak 1 were the level of background. (Data not shown). Considering the LC/MS/MS assay results described later, the radioactive peaks detected in the plasma and tumor at the retention times between 5 and 10 min were assumed to be one substance (SQAP), and thereafter were assessed as Peak 1 (Fig. 2 and Table 3). One hour after the administration, Peak 1 appeared to separate into several peaks (Fig. 2B and C). The peaks were mostly sulfoquinovosylpropanediol (SQP) or sulfoquinovose itself (Fig. 1D, E and Fig. S2) in which SQAP lost the fatty acid (C_{18}-stearic acid) with or without propanediol. The Peak 1 area in the tumor in Figure 2C also contained mainly SQP or sulfoquinovose at 8 h. However, there seemed to be many other compounds in that area as well (Fig. 2).

The results are shown in Figure 2 and Table 3 for the plasma and tumor. In the plasma, SQAP accounted for 89.6% of the radioactivity in the sample (1,997 ng/mL) at 5 min, 7.7% (53 ng/mL) at 1 h, and 2.5% (14 ng/mL) at 2 h after administration. SQAP was not detected at 4 h after administration (Fig. 2). A polar metabolite (Peak 1) in Figure 4 accounted for 6.0% of the sample radioactivity (134 ng eq./mL) at 5 min, 87.6% (600 ng eq./mL) at 1 h, 91.1% (509 ng eq./mL) at 2 h, 85.2% (239 ng eq./mL) at 4 h, and 64.8% (52 ng eq./mL) at 8 h after administration.

The results for the tumor are also shown in Figure 2 and Table 3. Five min after

administration, only SQAP was detected in the tumor, which accounted for 83.1% of the sample radioactivity (275 ng/g). SQAP accounted for 26.0% of the sample radioactivity (92 ng/g) at 1 h, 14.9% (56 ng/g) at 2 h, 12.1% (37 ng/g) at 4 h, and 9.7% (20 ng/g) at 8 h after administration. SQAP was not detected at 24 h after administration (Fig. 2). A polar metabolite (Peak 1) was not detected at 5 min after administration but accounted for 60.3% of the sample radioactivity (212 ng eq./g) at 1 h, 69.8% (260 ng eq./g) at 2 h, 76.5% (235 ng eq./g) at 4 h, 68.8% (141 ng eq./g) at 8 h, and 46.2% (35 ng eq./g) at 24 h after administration (Table 3).

Interestingly, the SQAP in the tumor did not degrade to the Peak 1 substance over longer times (Fig. 2 and Table 3). Just 1 h later, SQAP in the plasma remained only 7.7% of the administration, but a significant amount of SQAP (26%) remained in the tumor (Table 3). At 4 h, the radioactivity in the tumor (12.1%) was much larger than that in the plasma (Table 3). In both cases, the degradation product was mostly the Peak 1 substance within 4 h and then gradually fragmented to sulfoquinovose and the further metabolic products (Fig. 2 and Table 3).

In this study, 87.6% of [glucose-U-^{14}C]-SQAP (CP-3839) (Table 3, Peak 1 of Plasma at 1 h) was excreted as water-soluble metabolites, mainly SQP (See Quantification and identification of Peak1 in Supplement) 1.8% was SQAP itself together with the intestinal contents, and 7.0% was exhaled from the lung as $^{14}CO_2$. 95.8% of the total radioactivity administered was recovered as SQP in this test. The other non-labeled product, C_{18}-stearic acid, appeared to have been hydrolyzed.

LC/MS (MS/MS) Measurement of Plasma and Tumor

In LC/MS (MS^n) measurement of the reference standard SQAP, the MS chromatogram and MS and MS^n spectra were investigated (Table 4 and Fig. S2). The $[M–H]^-$ ion at *m/z* 567.3199 was found at the retention time of 49 min and resulted in fragment ions at *m/z* 283 and 225 (Table 4 and Fig. S2). Assignments of the fragment ions are shown in Figure 6. At *m/z* 283, SQAP appeared to be separated into SQP (Fig. 1D) and stearic acid and at *m/z* 225 to be degraded to sulfoquinovose (Fig. 1E) and additional compounds.

A comparison of the calculated and found mass data of the molecular formula and the *m/z* values of the metabolites identified or estimated in the plasma and tumor are shown in Figure 3 and Table 4. The difference between the calculated and found m/z was within ± 5 ppm. This suggests that the metabolites can be reliably identified by the mass measurement.

In the LC/MS (MS^n) measurements of the plasma and tumor, radio-chromatograms and MS chromatograms were investigated in the same manner (Fig. 3 and Table 4).

In the case of the plasma, an ion at *m/z* 301.0592 was detected from Peak 1, and the molecular formula was estimated as $C_9H_{17}O_9S$ (calculated value as $[M–H]^-$ ion: 301.0599) (Fig. 3 and Table 4). This mass number corresponded to the mass number of the parent compound (567–266). Because the fragment ion at *m/z* 225 was detected, the chemical structure was estimated to be a hydrolyzed metabolite. Assignment of the fragment ion is shown in Figure S2. An $[M–H]^-$ ion at *m/z* 567.3199 (calculated value as $[M–H]^-$ ion: 567.3208) was detected at the same retention time as SQAP (Fig. 3 and Table 4). Because the fragment ions were the same as those of the reference standard SQAP, this peak was identified as the parent compound.

A radiochromatogram and MS-chromatogram from the LC/MS (MS^n) measurement of the tumor are also shown in Table 4 and Fig. 3, respectively. Because an ion at *m/z* 301.0588 was detected from Peak 1 similar to that from Peak 1 in the plasma (Fig. 3 and Table 4), and the fragmented ions were similar to those of Peak 1 in the plasma, the peak was considered to be an identical metabolite. An $[M–H]^-$ ion at *m/z* 567.3193 was detected from the peak at the same retention time as that of SQAP. Because the fragmented ions were the same as those of the reference standard SQAP, this peak was identified as the parent compound (See Quantification and identification of Peak1 in Supplement).

These results indicated that the metabolic process of SQAP *in vivo* was the same in either the plasma or tumor, and the speed in the plasma was fast.

Whole-body Autoradiography (Tissue Distribution)

In the ADME tests using 1,3-propanediol[1-^{14}C]-SQAP (CP-3635), the radioactivity concentrations in the plasma and tumor were analyzed after intravenous administration of 1 mg (3.48 MBq)/kg of 1,3-propanediol[1-^{14}C]-SQAP (CP-3635) to non-fasting Lu65 transplanted male nude mice. Analysis showed that the 1,3-propanediol[1-^{14}C]-SQAP (CP-3635)-derived radioactivity accumulated in the tumor (Fig. 4 and Table 5). Some mechanisms can be deduced as follows. One possibility is that SQAP was metabolized preferentially and more slowly in the tumor than in the plasma. The other possibilities are enhanced uptake of SQAP or slower excretion of SQAP. Another possibility can be also deduced. Our results also suggested that SQAP was caught in necrotic areas of the tumor where blood flow did not allow for the faster clearance of radioactivity, because SQAP in the tumor continually kept much higher level than those in brain and testis. The information about ADME of SQAP is clinically important for the development of a radiosensitizer.

For further study, whole-body autoradiography for total radioactivity derived from 1,3-propanediol[1-^{14}C]-SQAP (CP-3635) was performed. Figure 4 shows an autoradiographic image taken on the median line along the mouse whole body. The amounts in Table 5 were measured by autoluminography, which does not allow for correction of background blood or urine in the tubules. Table 5 and Figure 4 show photo-stimulated luminescence (PSL) per unit area in tissues at 5 min, 1 hour, 2 h, 4 h, 8 h, 24 h, 72 h, or 168 h after a single intravenous administration of 1,3-propanediol[1-^{14}C]-SQAP (CP-3635) to non-fasting male KSN-mice (dose: 1 mg/kg as SQAP), respectively (Fig. 4 and Table 5). For each time point in Table 5, two non-fasting male KSN-mice were used. The distribution was almost the same in the two mice. Table 5 presents the mean values of the two mice.

Autoradiographic data indicated that 1,3-propanediol[1-^{14}C]-SQAP (CP-3635)-derived radioactivity was widely distributed at first throughout the organs and tissues in the male KSN-mice (Fig. 4 and Table 5). Interestingly, the photo-stimulated luminescence showed that

SQAP was relatively difficult to distribute in the brain and testis and that the radioactivity did not remain long in any organ (Fig. 4 and Table 5).

At 5 min post dose (end of infusion), the highest photo-stimulated luminescence occurred in the liver, with SQAP being two-fold higher concentration than that in blood, and it was almost the same level as that in blood in the adrenal gland and lung (Fig. 4 and Table 5). The radioactivity levels in the kidney, spleen, heart, and other organs were lower than that in blood (Table 5 and Fig. 4). The radioactivity level was also not high in the tumor (Fig. 4 and Table 5).

At 1 h, the highest radioactivity levels were in the urinary bladder and the second highest level was in the liver (Fig. 4 and Table 5). The radioactivity levels in the bile of the gall bladder and kidney were also very high. In contrast, the radioactivity level in blood was much lower (Fig. 4 and Table 5). In the other organs, the radioactivity levels were lower than that in blood (Fig. 4 and Table 5). The values became much higher in the excretory organs and their excreted liquids, a tendency that continued later (Table 5). SQAP was rapidly accumulated in the liver and kidney, and was soon metabolized and excreted (Table 5). The only exception was the tumor. The photo-stimulated luminescence increased although the value was not high (Table 5). The radioactivity mostly came from the metabolic products (SQP and sulfoquinovose in Fig. 1D and E), which was also observed in the plasma (our unpublished data).

At 2 h, the values in the urinary bladder and the liver became extremely high. On the other hand, SQAP was mostly disappeared within 2 hours in the most organs (Fig. 4 and Table 5).

At 4 h, the radioactivity levels had greatly decreased in most organs except in the tumor and excretory organs, including excreta (Fig. 4 and Table 5). In the excretory organs or the excreta (e.g., urinary bladder, urine, intestinal contents, and gall bladder bile) the radioactivity increased dramatically (Fig. 4 and Table 5). In the process, although the luminescence values in the lung, blood, adrenal gland, and kidney rapidly decreased, those in the kidney and liver remained very high (Fig. 4 and Table 5). It appeared that SQAP actively gathered from the entire body and broke down to SQP and other compounds.

At 8 h, only the tumor showed more than a two-fold higher radioactivity level than the levels in any other organs except in the excretory organs and excreta (Table 5). As suggested in Figure 4 and Table 3, the radioactivity of SQAP appeared to be relatively larger in the tumor. Intra-organ differential distribution was apparent in Lu65 tumor transplanted in the back of the mice, in which the luminescence unevenly increased in the tumor. Generally, the tissue radioactivity concentrations decreased over time, but elimination was not complete at 72 h post dose (Fig. 4 and Table 5). At 168 h, the radioactivity had been completely eliminated (Fig. 4).

ACKNOWLEDGMENTS

This work was supported by the Program for Promotion of Fundamental Studies in Health Science of the National Institute of Biomedical Innovation (NiBio), Japan.

Disclosure of Potential Conflicts of Interest

There are no potential conflicts of interest related to this work to disclose.

Authors' Contributions

Conception and design: H. Sahara, M. Miura, F. Sugawara, K. Sakaguchi.

Acquisition of biological data (e.g., provided animals, provided facilities): T. Ruike, Y. Kanai, K. Iwabata, Y. Matsumoto, M. Ishima, K. Ohta, M. Oshige, S. Katsura, H. Sahara, M. Miura, K. Sakaguchi.

Biological analysis and interpretation of data (e.g., LC-MS data analysis, computational analysis): M. Ishima, K. Ohta, M. Miura, F. Sugawara, K. Sakaguchi.

Chemical Synthesis (e.g., organic synthesis, NMR and MS data collection, structural analysis): T. Ruike, Y. Kanai, H. Murata, K. Kuramochi, S. Kamisuki, F. Sugawara.

Writing, review, and/or revision of the manuscript: M. Oshige, K. Katsura, F. Sugawara, K. Sakaguchi.

Administrative, technical, or material support (e.g., reporting or organizing data, constructing databases): H. Murata, M. Ishima, K. Ohta, F. Sugawara, K. Sakaguchi.

Study supervision: M. Miura, F. Sugawara, K. Sakaguchi.

REFERENCES

Aoki S, Ohta K, Yamazaki T, Sugawara F, Sakaguchi K (2005) Mammalian mitotic centromere-associated kinesin (MCAK), a new molecular target of sulfoquinovosylacylglycerols (SQAGs), novel anti-tumor and immunosuppressive agents. *FEBS J* **272**:2132-2140

Aoki S, Matsumoto K, Ohta K, Sakai H, Abe M, Miura M, Sugawara F, Sakaguchi K (2006) An emulsion of sulfoquinovosylacylglycerol and long-chain alkane increases its permeability in tumor cells. *J Membrane Biol* **213**:11-18

Bowsher, JE, Hedlund LW, Wong T, Dewhirst MW (2006) Intertumoral Differences in Hypoxia Selectivity of the PET Imaging Agent 64Cu(II)-Diacetyl-Bis(N4-Methylthiosemicarbazone). *J Nucl Med* **47**:989-998

Hanashima S, Mizushina Y, Ohta K, Yamazaki T, Sugawara F, Sakaguchi K (2000a) Structure-activity relationship of a novel inhibitor group of mammalian DNA polymerases, synthetic sulfoquinovosylacylglycerols. *Jpn J Cancer Res* **91**:73-83

Hanashima S, Mizushina Y, Yamazaki T, Ohta K, Takahashi S, Koshino H, Sahara H, Sakaguchi K, Sugawara F (2000b) Structural determination of sulfoquinovosyldiacylglycerol by chiral synthesis. *Tetrahedron Lett* **41**:4403-4407

Hanashima S, Mizushina Y, Yamazaki T, Ohta K, Takahashi S, Sahara H, Sakaguchi K, Sugawara F (2001) Synthesis of sulfoquinovosylacylglycerols, inhibitors of eukaryotic DNA polymerase α and β. *Bioorg Med Chem* **9**:367-376

Herman TS, Teicher BA, Dewhirst MW, Zimmerman D (1990) Rate of infusion: an important factor in circulatory effects of perfluorochemical emulsions (PFCES). *Int J Radiat Oncol Biol Phys* **19**:136

Iwamoto H, Nakamura T, Koga H, Izaguirre-Carbonell J, Kamisuki S, Sugawara F, Abe M, Iwabata K, Ikezono Y, Sakaue T, Masuda A, Yano H, Ohta K, Nakano M, Shimose S, Shirono T, Torimura T (2015) Inhibition of hypoxia-inducible factor via upregulation of von

Hippel-Lindau protein induces "angiogenic switch off" in a hepatoma mouse model. *Mol Ther Oncolytics* **2**: 15020

Izaguirre-Carbonell J, Murata H, Ohta K, Kusayanagi T, Tsukuda S, Iwabata K, Kanai Y, Kamisuki S, Sakaguchi K, Sugawara F (2014) Identification and study of SQAP-binding proteins from a T7 phage display screen. *Planta Med* **80**:PH4

Izaguirre-Carbonell J, Kawakubo H, Murata H, Tanabe A, Takeuchi T, Kusayanagi T, Tsukuda S, Hirakawa T, Iwabata K, Kanai Y, Ohta K, Masahiko M, Sakaguchi K, Matsunaga S, Sahara H, Kamisuki S, Sugawara F (2015) Novel anticancer agent, SQAP, binds to focal adhesion kinase and modulate its activity. *Nat Commun* **5**:15136

Miura M, Sakimoto I, Ohta K, Sugawara F, Sakaguchi K (2007) Sulfoglycolipids as candidate antiangiogenetic radiosensitizers (a review). *Anticancer Drugs* **18**:1-5

Mizushina Y, Yagi H, Tanaka N, Kurosawa T, Seto H, Katsumi K, Onoue M, Ishida H, Iseki A, Nara T, Morohashi K, Horie T, Onomura Y, Narusawa M, Aoyagi N, Takami K, Yamaoka M, Inoue Y, Matsukage A, Yoshida S, Sakaguchi K (1996) Screening of inhibitor of eukaryotic DNA polymerases produced by microorganisms. *J Antibiot (Tokyo)* **49**:491-492

Mizushina Y, Watanabe I, Ohta K, Takemura M, Sahara H, Sugawara F, Matsukage A, Yoshida S, Sakaguchi K (1997) AIDS-antiviral sulfolipids from a pteridophyta, Athyrium niponicum, are selective inhibitors of Mammalian DNA polymerase α and β, but not of HIV reverse transcriptase. *Biochem Pharmacol* **55**:537-541

Ohta K, Mizushina Y, Hirata N, Takemura M, Sugawara F, Matsukage A, Yoshida S, Sakaguchi K (1998) Sulfoquinovosyldiacylglycerol, KM043, a new potent inhibitor of eukaryotic DNA Polymerases and HIV-Reverse Transcriptase 1 from A Marine Red Alga, *Gigartina tennella*. *Chem Pharm Bull (Tokyo)* **46**:684-486

Ohta K, Mizushina Y, Hirata N, Takemura M, Sugawara F, Matsukage A, Yoshida S, Sakaguchi K (1999) Studies on action of sulfoquinovosyldiacylglycerol, a new mammalian DNA polymerase inhibitor, from a sea alga, *Gigartina tenella*. *Biol Pharm Bull* **22**:111-116

Ohta K, Hanashima S, Mizushina Y, Yamazaki T, Saneyoshi M, Sugawara F, Sakaguchi K (2000) Studies on a novel DNA polymerase inhibitor group, synthetic sulfoquinovosylacylglycerols: inhibitory action on cell proliferation. *Mutat Res* **467**:139-152

Ohta K, Mizushina Y, Yamazaki T, Hanashima S, Sugawara F, Sakaguchi K (2001) Specific interaction between oligosaccharide on tumor cell surface and novel antitumor agents, sulfoquinovosylmonoacylglycerols. *Biochem Biophys Res Commun* **288**:893-900

Ohta K, Murata H, Mori Y, Ishima M, Sugawara F, Sakaguchi K, Miura M (2010) Remodeling of the tumor microenvironment by combined treatment with a novel radiosensitizer, α-sulfoquinovosylmonoacylglycerol (α-SQMG) and X-irradiation. *Anticancer Res* **30**:4397-4404

Sakimoto I, Ohta K, Yamazaki T, Ohtani S, Sahara H, Sugawara F, Sakaguchi K, Miura M (2006) α-Sulfoquinovosylmonoacylglycerol (α-SQMG) is a novel potent radiosensitizer targeting tumor angiogenesis. *Cancer Res* **66**:2287-2295

Sakaguchi K, Sugawara F (2008) New cancer chemotherapy agents: Inhibitors of DNA polymerase (a review)**.** *Current Drug Therapy* **3**:44-53

Sakaguchi K (2015) A prospect of a new potent radiosensitizer SQAG/SQAP (a review in Japanese). *Radiat Biol Res Commun* **50**:1-17

Sawada Y, Omoto K, Kohei H, Sakaguchi K, Miura M, Tanabe K (2015) Sulfoquinovosylacylpropanediol is a novel potent radiosensitizer in prostate cancer. *Int J Urol* **22**:590-595

Takakusagi Y, Takakusagi K, Sugawara F, Sakaguchi K (2010) Use of phage display technology for the determination of the targets for small-molecule therapeutics (a review). *Expert Opin Drug Discov* **5**:361-389

Takakusagi Y, Takakusagi K, Ida N, Takami M, Matsumoto Y, Kusayanagi T, Nakabayashi T, Aoki S, Murata H, Ohta K, Sugawara F, Sakaguchi K (2011) Binding region and interaction properties of sulfoquinovosylacylglycerol (SQAG) with human vascular endothelial growth

factor 165 revealed by biosensor-based assays. *MedChemComm* **2**:1188-1193

Takakusagi Y, Matsumoto S, Saito K, Matsuo M, Takakusagi K, Kishimoto S, Ishima M, Murata H, Ohta K, Miura M, Sugawara F, Sakaguchi K, Mitchell JB, Krishna MC (2015) Increase in tumor oxygenation and radiosensitivity caused by SQAP (CG-0321): the mechanism of actions revealed by *in vivo* imaging studies. ICRR (15th International Congress of Radiation Research) 3-PS2E-27

Yuan H., Schroeder T, Bowsher JE, Hedlund LW, Wong T, Dewhirst MW (2006) Intertumoral Differences in Hypoxia Selectivity of the PET Imaging Agent ^{64}Cu(II)-Diacetyl-Bis(N^4-Methylthiosemicarbazone). *J Nucl Med* **47**:989-998

Figure 1

Structures of A: Sulfoquinovosylacylglycerol (SQAG) (R=OH) and Sulfoquinovosylacylpropanediol (SQAP) (R=H) (Lot No. CG-0321), B: 1,3-propanediol[1-^{14}C]-SQAP (C18:0) (Lot No. CP-3635) (An asterisk mark references the [^{14}C] position) (Lot No. CP-3635), C: [Glucose-U-^{14}C]-SQAP (C18:0) (Lot No. CP-3839) (Asterisk marks references the [^{14}C] position), D: Sulfoquinovosylpropanediol (SQP) and E: Sulfoquinovose.

A

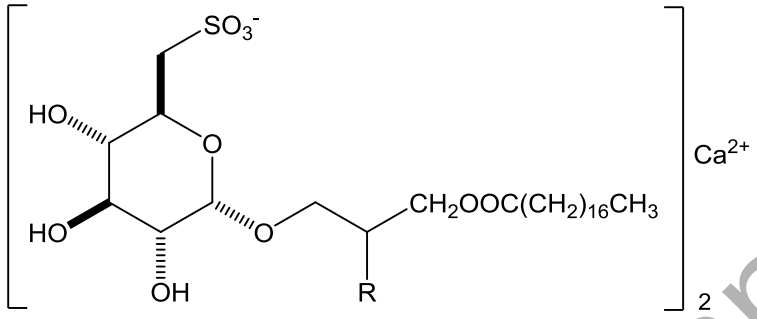

B

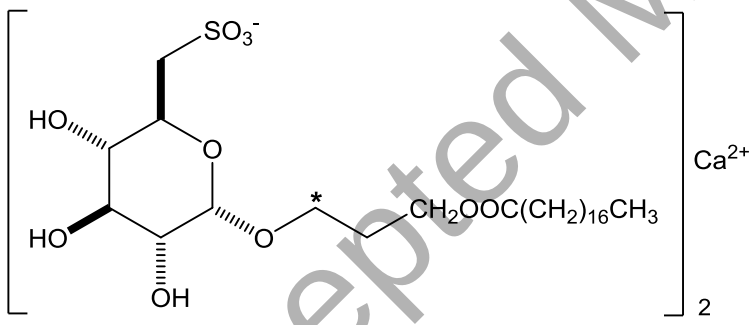

C

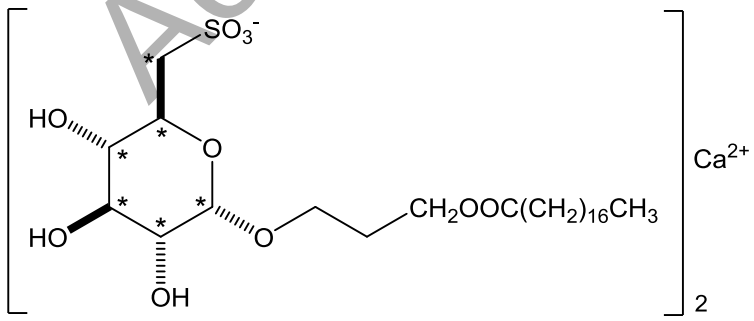

D

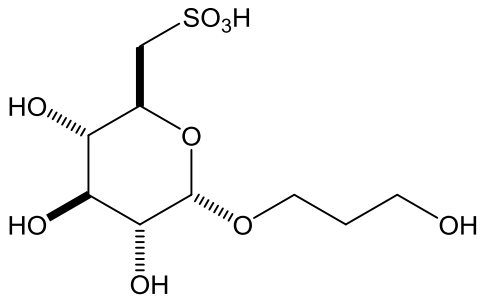

E

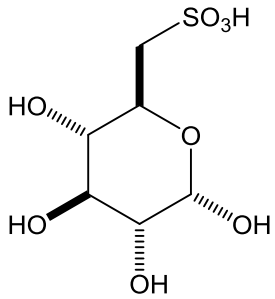

Figure 2

HPLC radiochromatogram of [Glucose-U-^{14}C]-SQAP (CP-3839) (A), plasma (B) and tumor (C) after a single intravenous administration of [Glucose-U-^{14}C]-SQAP (CP-3839) to non-fasting Lu65 transplanted male nude mice (dose: 2 mg (2.98 MBq)/kg as SQAP).

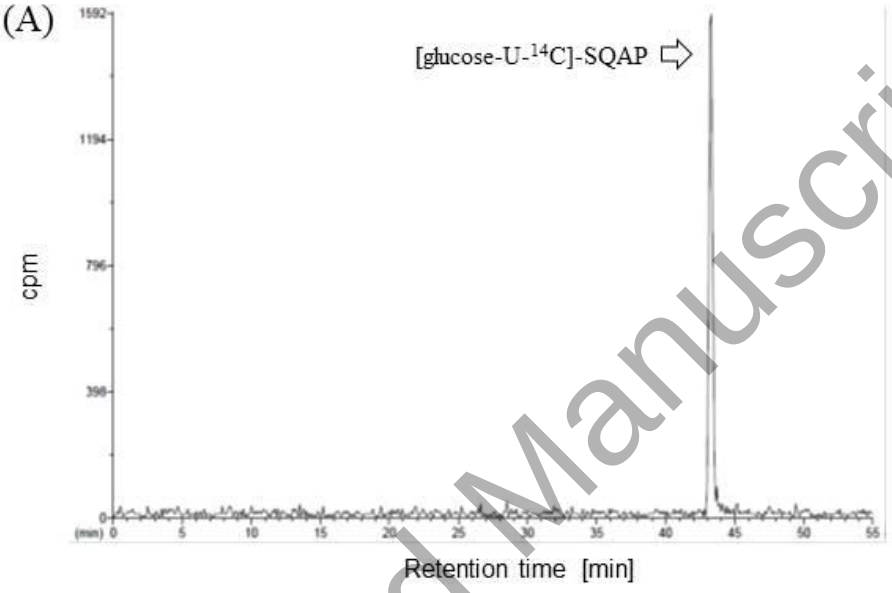

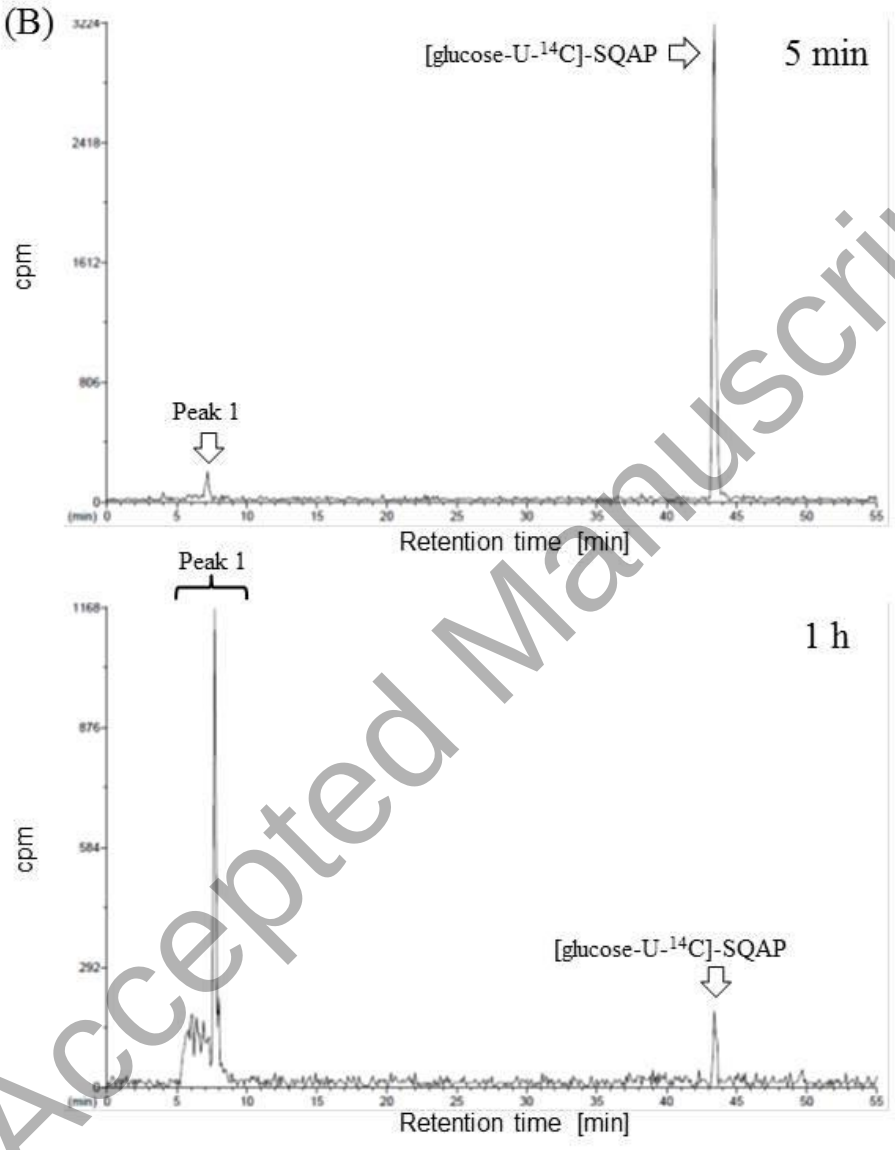

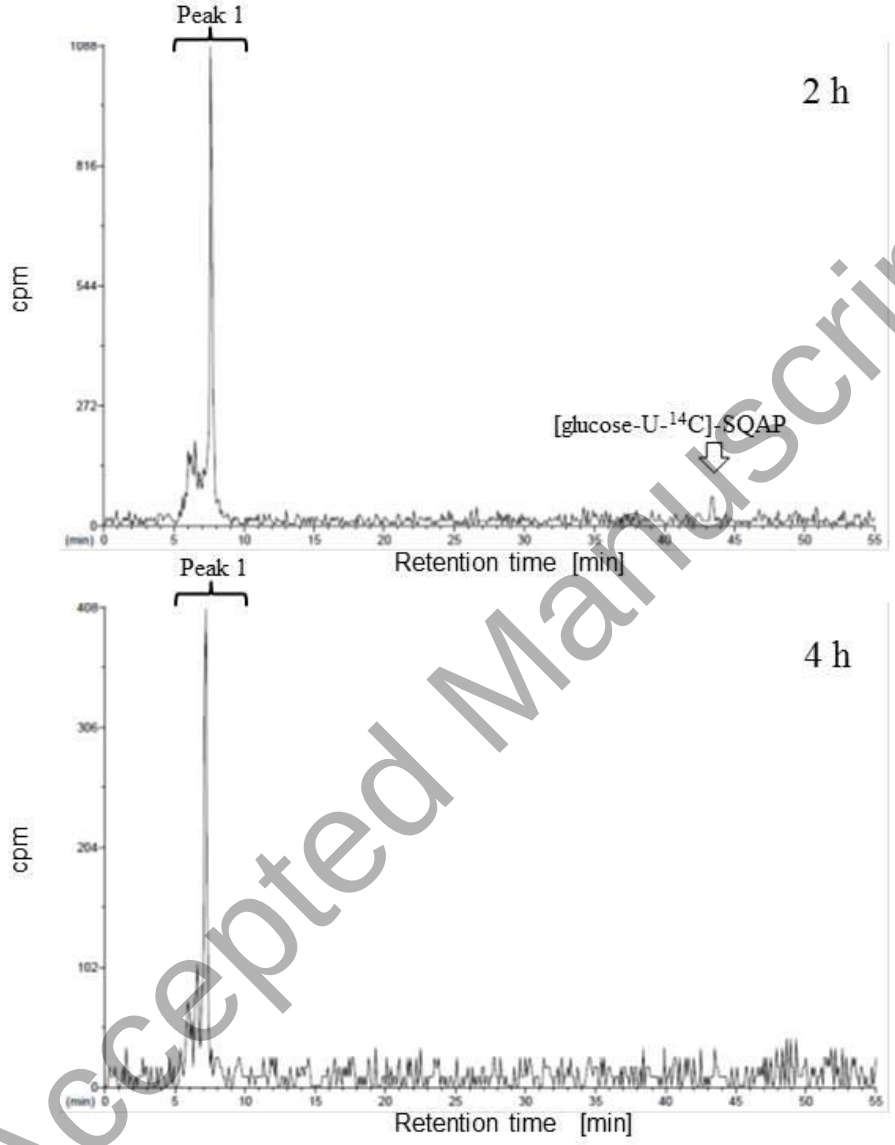

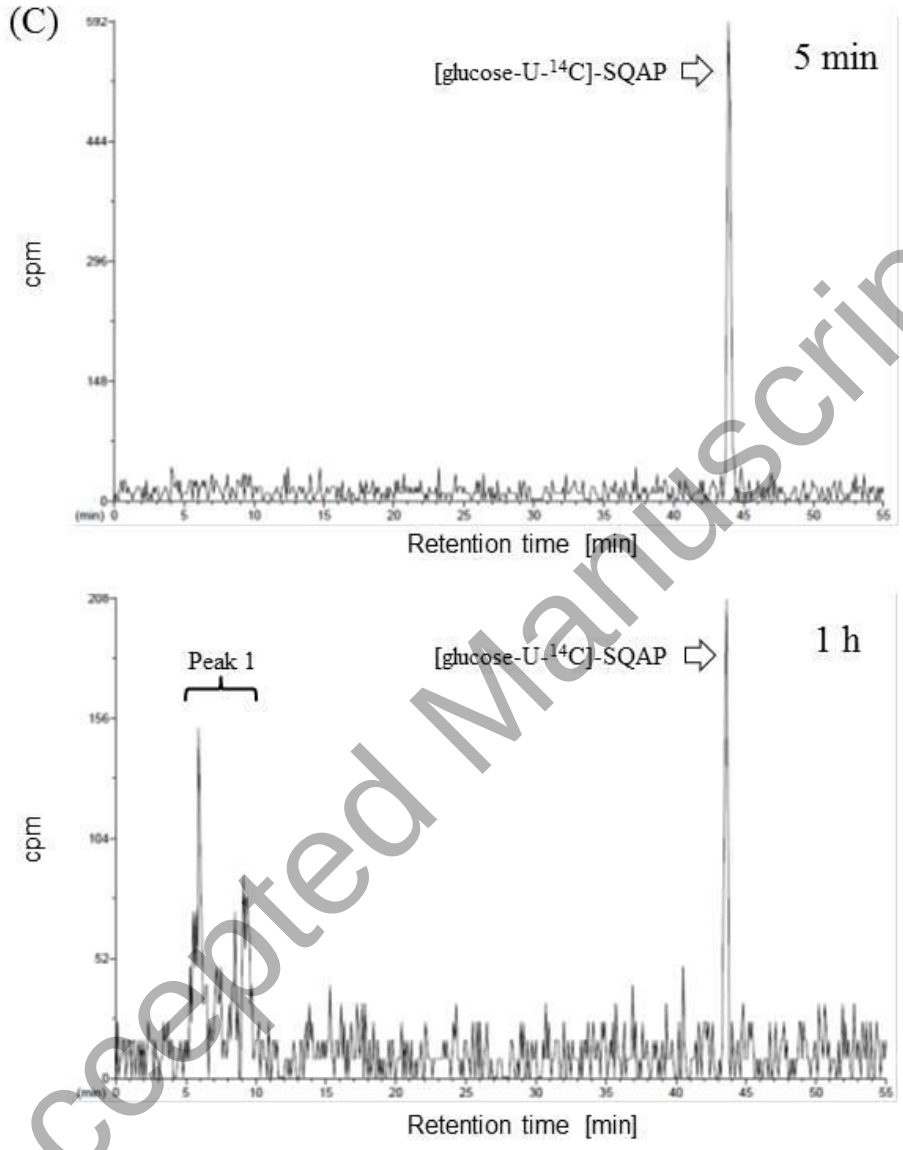

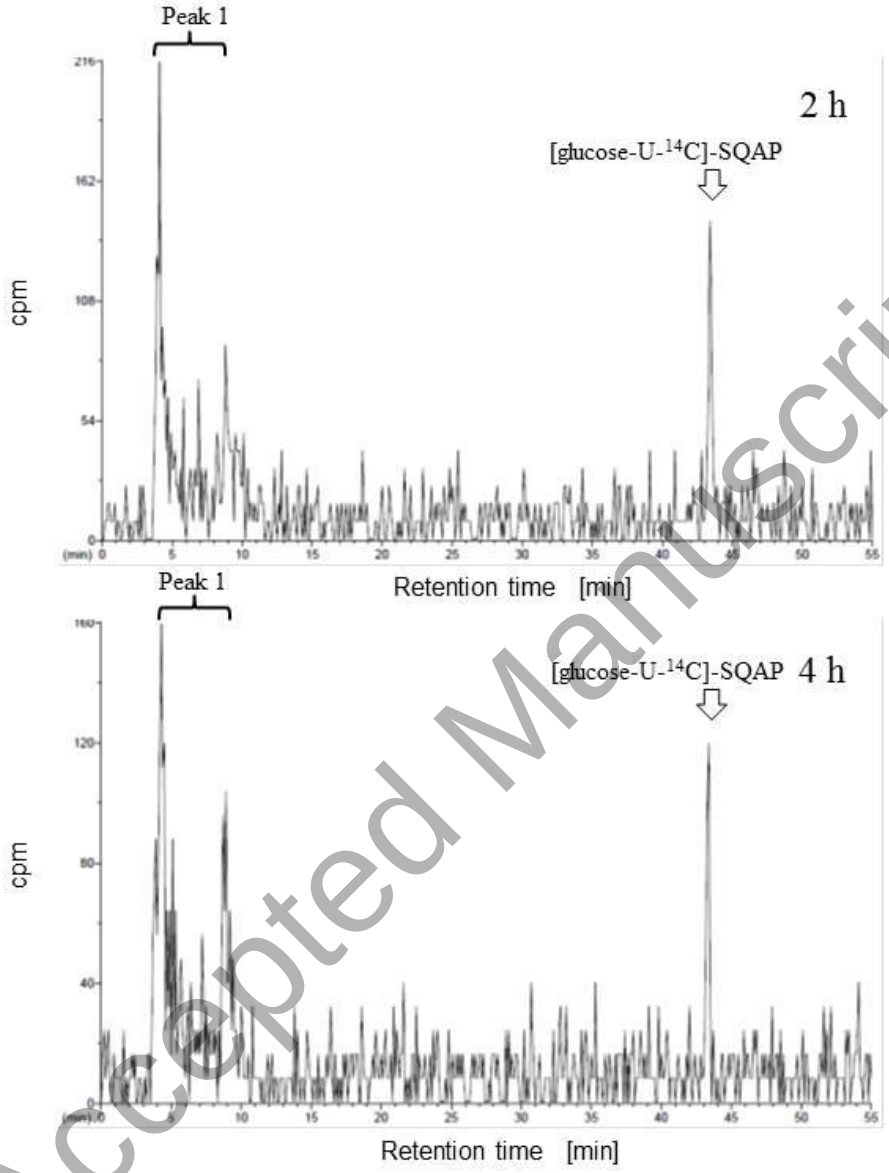

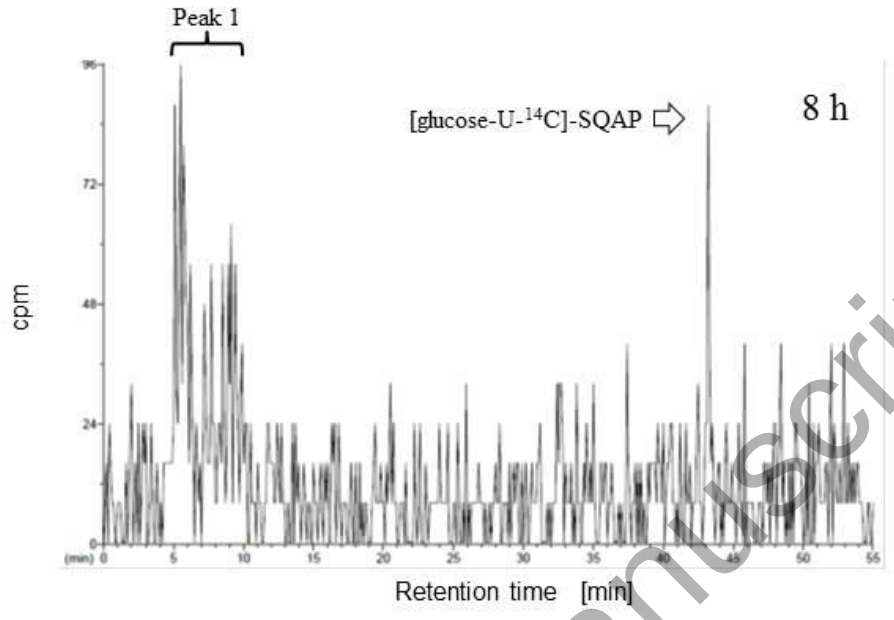

Figure 3

HPLC radiochromatogram acquired concurrently with LC/MS^n measurement of plasma 1 h after a single intravenous administration of [glucose-U-^{14}C]-SQAP (CP-3839) to non-fasting Lu65 transplanted male nude mice (dose: 2 mg (2.98 MBq)/kg as SQAP).

(A) ESI (-) mass chromatograms of plasma, 1 h after a single intravenous administration of [glucose-U-^{14}C]-SQAP (CP-3839) to non-fasting Lu65 transplanted male nude mice (dose: 2 mg (2.98 MBq)/kg as SQAP).

(B) ESI (-) MS and MS^2 spectra of [glucose-U-^{14}C]-SQAP (CP-3839) in tumor, 1 h after a single intravenous administration of [glucose-U-^{14}C]-SQAP (CP-3839) to non-fasting Lu65 transplanted male nude mice (dose: 2 mg (2.98 MBq)/kg as SQAP). (Top): total ion current chromatogram (TICC) of the extract, (middle): peak1 at *m/z* 301 was detected from the TICC, (bottom): non-radioactive SQAP at *m/z* 567 was detected from the TICC.

(A)

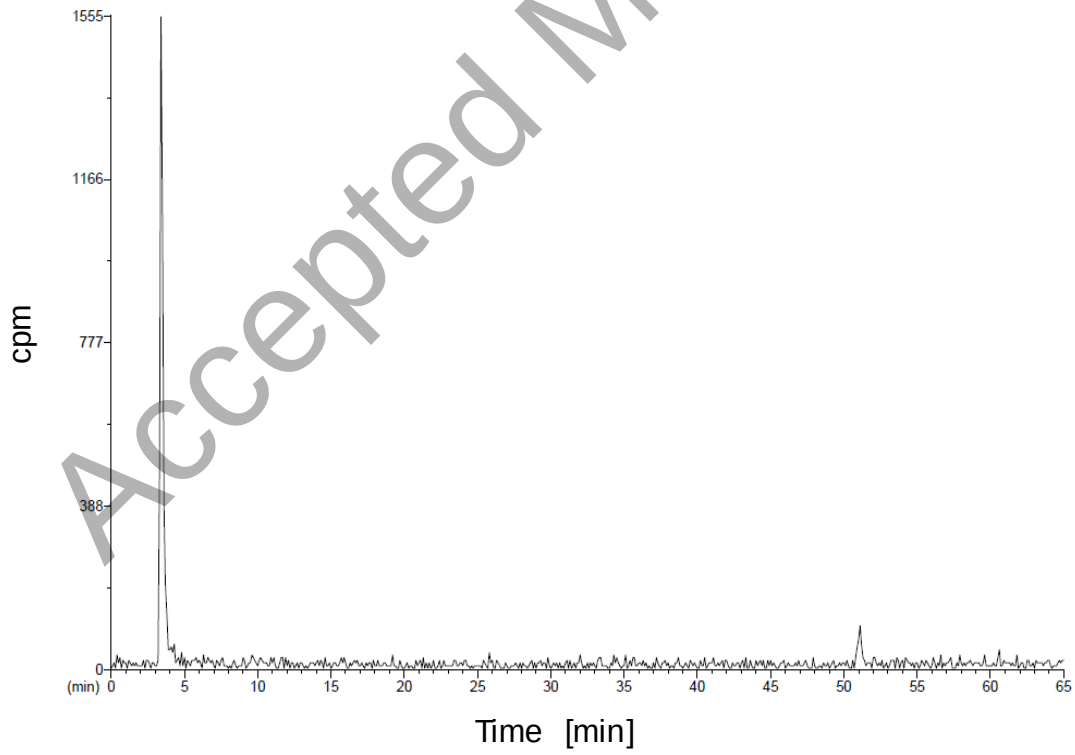

(B)

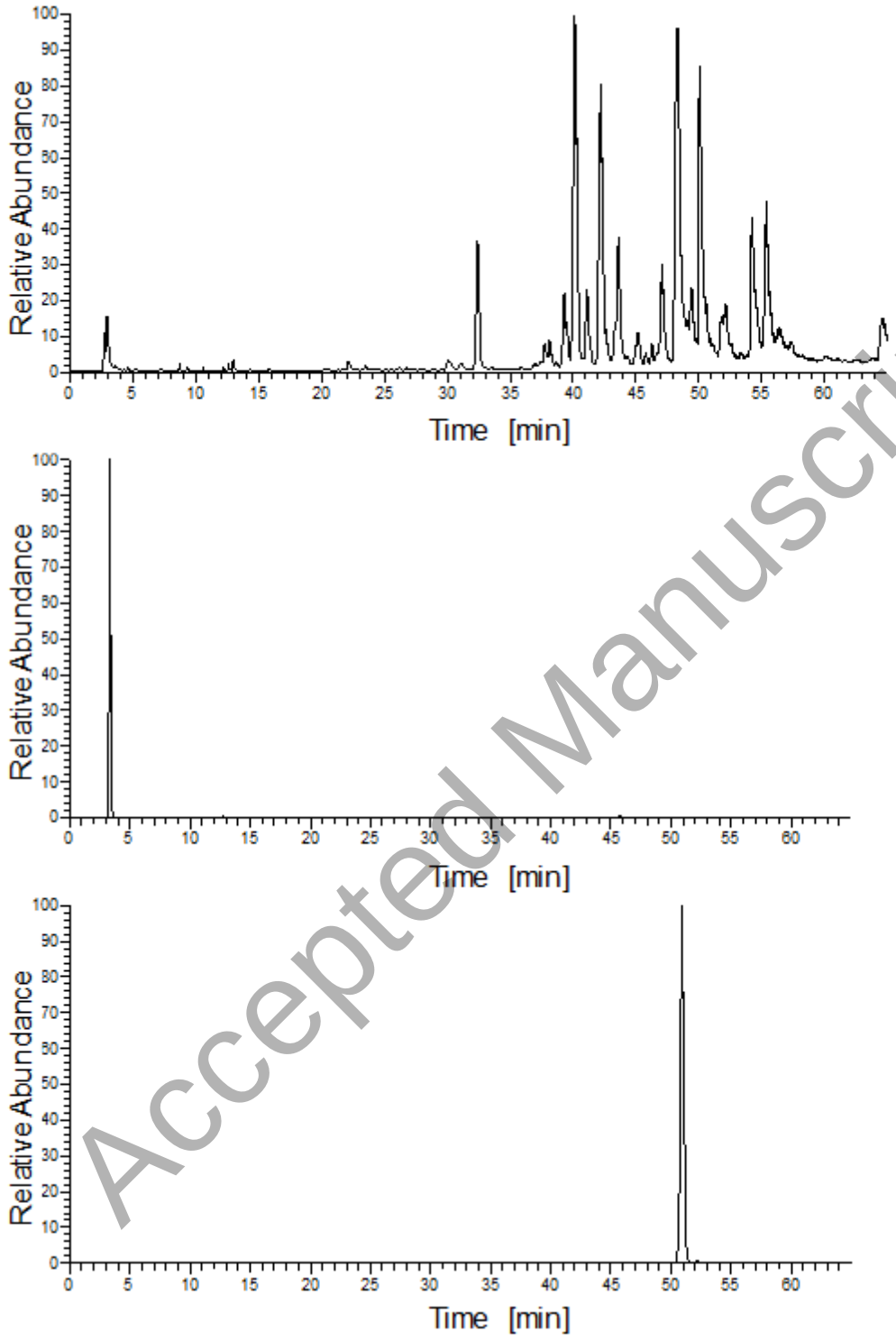

Figure 4

Whole-body radioluminograms after a single intravenous administration of 1,3-propanediol[1-^{14}C]-SQAP (CP-3635) to a non-fasting male KSN-mouse (dose: 1 mg (3.49 MBq)/kg); these show the central-axis aspect of the body of the mouse.

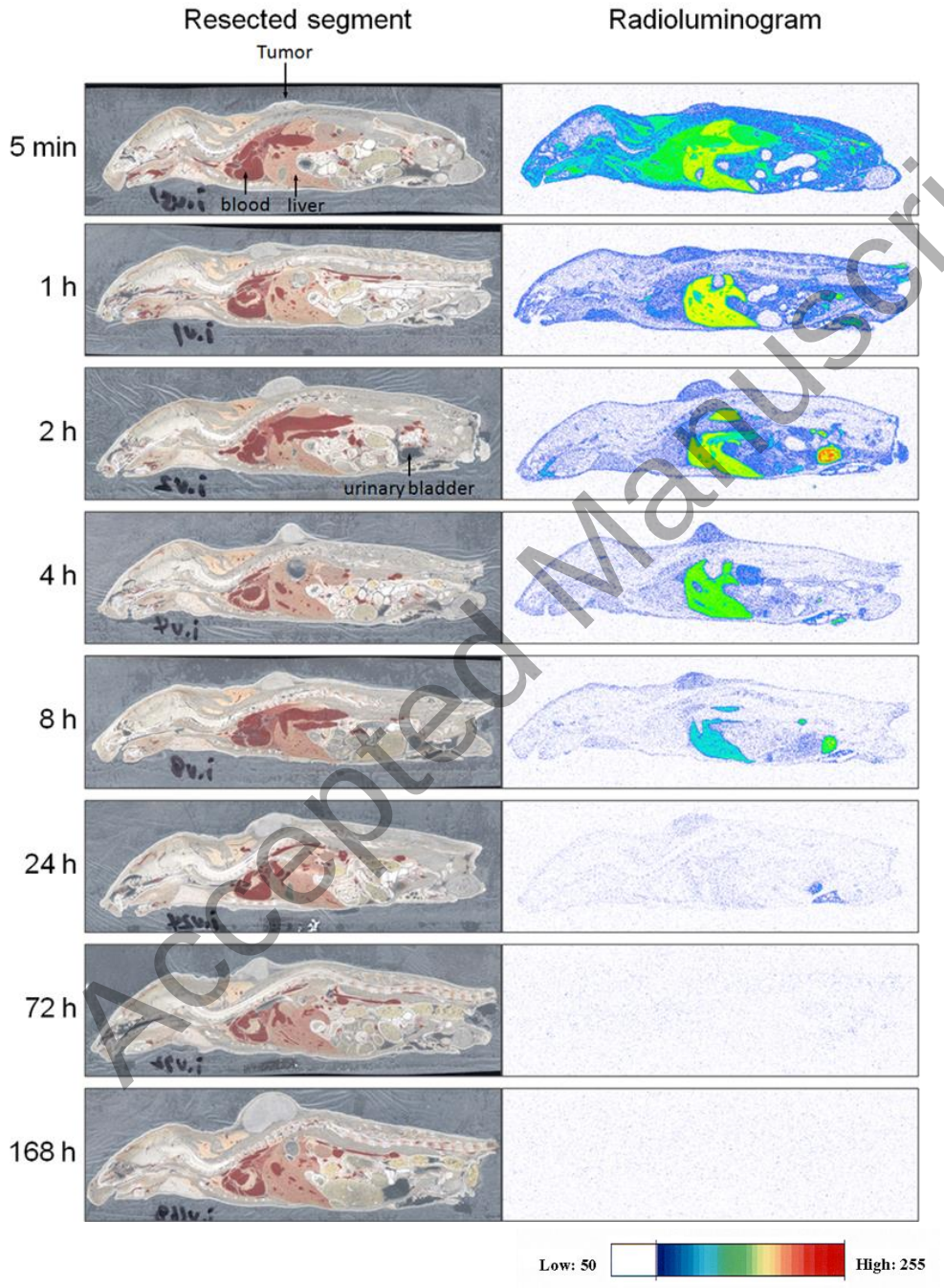

Table 1

Radioactivity concentrations in plasma and tumor after a single intravenous administration of [glucose-U-^{14}C]-SQAP (CP-3839) to non-fasting Lu65 transplanted male nude mice (dose: 2 mg (2.98 MBq)/kg as SQAP).

	Radioactivity concentration (ng eq. of SQAP/g or mL)	
Time	Plasma	Tumor
5 min	2229 ± 51	331 ± 29
1 h	685 ± 221	352 ± 42
2 h	559 ± 32	373 ± 35
4 h	281 ± 65 *	307 ± 33 *
8 h	81 ± 18 †	205 ± 25 †
24 h	4 ± 1 ‡	75 ± 4 ‡
PK Parameters	Plasma	Tumor
$t_{1/2}$ (h)	3.1 (1–24 h)	10 (4–24 h)
$AUC_{0\text{-}24\ h}$ (ng eq.·h/g or mL)	4400	4630
$AUC_{0\text{-}\infty}$ (ng eq.·h/g or mL)	4420	5730

Figures in parentheses represent time ranges for calculation. Radioactivity concentration data are expressed as the mean values ± SD of three animals. PK parameter data are calculated from the mean concentrations of three animals. The asterisk (*) denotes no significant differences in the radioactive concentrations of plasma and tumor. The dagger (†) and the double dagger (‡) denote a statistically significant difference in the radioactive concentrations of plasma and tumor (paired t-test, $p < 0.05$).

Table 2

The individual sample recovery as a percentage of doses from plasma and tumor after a single intravenous administration of [glucose-U-^{14}C]-SQAP (CP-3839) to non-fasting Lu65 transplanted male nude mice (dose: 2 mg (2.98 MBq)/kg as SQAP).

Sample	Time	Recovery of radioactivity (%)
Plasma	5 min	94.2
	1 h	95.1
	2 h	89.2
	4 h	86.7
	8 h	102.0
Tumor	5 min	102.2
	1 h	99.2
	2 h	95.0
	4 h	93.9
	8 h	91.3
	24 h	107.1

Data were obtained from the pooled samples of three animals.

Table 3

Composition of radioactivities in plasma and tumor after a single intravenous administration of [glucose-U-^{14}C]-SQAP (CP-3839) to non-fasting Lu65 transplanted male nude mice (dose: 2 mg (2.98 MBq)/kg as SQAP).

Plasma

	% in sample				
Metabolite	5 min	1 h	2 h	4 h	8 h
Peak 1	6.0	87.6	91.1	85.2	64.8
SQAP	89.6	7.7	2.5	N.D.	N.D.
Others	4.4	4.7	6.4	14.8	35.2

	Concentration (ng eq. of SQAP/mL)				
Metabolite	5 min	1 h	2 h	4 h	8 h
Peak 1	134	600	509	239	52
SQAP	1997	53	14	N.D.	N.D.
Total conc.	2229	685	559	281	81

Tumor

	% in sample					
Metabolite	5 min	1 h	2 h	4 h	8 h	24 h
Peak 1	N.D.	60.3	69.8	76.5	68.8	46.2
SQAP	83.1	26.0	14.9	12.1	9.7	N.D.
Others	16.9	13.7	15.3	11.4	21.5	53.8

	Concentration (ng eq. of SQAP/g)					
Metabolite	5 min	1 h	2 h	4 h	8 h	24 h
Peak 1	N.D.	212	260	235	141	35
SQAP	275	92	56	37	20	N.D.
Total conc.	331	352	373	307	205	75

Data were obtained from the pooled samples of three animals.

N.D.: Not detected.

Table 4

Summary of accurate mass data of plasma and tumor 1 h after a single intravenous administration of [glucose-U-^{14}C]-SQAP (CP-3839) to non-fasting Lu65 transplanted male nude mice (dose: 2 mg (2.98 MBq)/kg as SQAP).

Plasma

	Molecular formula	Accurate mass (*m/z*)		Δ		Mass shift	Estimated metabolism
	$[M-H]^-$	calcd	found	Da	ppm		
Peak 1	$C_9H_{17}O_9S$	301.0599	301.0592	−0.0007	−2.33	−266	Hydrolysis
SQAP	$C_{27}H_{51}O_{10}S$	567.3208	567.3199	−0.0009	−1.59	-	-

ppm = [found value / calculated value–1] × 10^6

Tumor

	Molecular formula	Accurate mass (*m/z*)		Δ		Mass shift	Estimated metabolism
	$[M-H]^-$	calcd	found	Da	ppm		
Peak 1	$C_9H_{17}O_9S$	301.0599	301.0588	−0.0011	−3.65	−266	Hydrolysis
SQAP	$C_{27}H_{51}O_{10}S$	567.3208	567.3193	−0.0015	−2.64	-	-

ppm = [found value / calculated value–1] × 10^6

Table 5

Levels of total radioactivity in tissues after a single intravenous administration of 1,3-propanediol[1-^{14}C]-SQAP (CP-3635) to non-fasting male KSN-mice (dose: 1 mg (3.49 MBq)/kg). Each value is the average of data from two mice. N.S.: Not specified.

PSL/mm^2

Tissue	5 min	1 hour	2 hours	4 hours	8 hours	24 hours	72 hours
Adrenal gland	48.45	5.95	3.18	3.09	1.64	N.S.	N.S.
Bile in gall bladder	4.03	18.42	19.03	14.70	6.27	N.S.	N.S.
Blood	40.51	5.16	2.74	1.80	0.46	0.12	N.S.
Bone marrow	18.51	3.35	2.07	1.52	1.19	0.47	N.S.
Brain	2.06	0.80	0.71	0.54	0.33	0.08	N.S.
Brown fat	24.05	2.10	1.01	0.89	0.48	0.33	N.S.
Epididymis	4.65	5.70	4.36	1.72	1.41	0.92	N.S.
Eyeball	1.18	0.71	0.57	0.51	0.22	N.S.	N.S.
Fat	6.93	0.61	0.42	0.38	0.14	N.S.	N.S.
Gastric contents	N.S.	0.87	0.99	1.02	0.25	N.S.	N.S.
Harderian gland	8.76	3.74	3.67	3.28	2.01	0.55	N.S.
Heart	40.31	2.24	1.18	1.20	0.31	0.16	N.S.
Intestinal contents	N.S.	8.06	12.32	16.79	3.83	N.S.	N.S.
Intestine	9.99	4.10	3.26	1.67	0.96	0.24	N.S.
Kidney	32.08	33.04	42.06	27.87	15.81	0.28	N.S.
Liver	85.51	135.77	106.77	67.40	17.24	0.43	N.S.
Lung	68.06	5.31	3.57	3.81	1.47	0.77	N.S.
Mandibular gland	9.20	4.48	1.84	1.41	0.90	0.34	N.S.
Pancreas	11.35	2.66	2.61	1.51	0.66	0.11	N.S.
Pituitary gland	19.04	3.22	1.55	1.23	1.57	N.S.	N.S.
Preputial gland	6.54	6.68	5.27	5.85	4.86	2.50	0.35
Skeletal muscle	5.44	1.08	0.48	0.31	0.11	0.09	N.S.
Skin	5.50	3.61	1.80	1.64	0.89	0.26	N.S.
Spleen	24.09	3.51	2.00	1.67	1.23	0.67	N.S.
Stomach	14.89	4.76	3.60	2.21	1.24	0.26	N.S.
Testis	1.24	1.42	1.06	0.93	0.54	0.25	N.S.
Thyroid gland	21.26	2.78	1.43	0.89	0.65	0.24	N.S.
Tumor	**2.28**	**4.16**	**2.82**	**2.76**	**1.79**	**0.59**	N.S.
Urinary bladder	5.33	299.25	552.40	111.56	131.26	2.23	N.S.
Urine in bladder	N.S.	202.24	532.17	308.83	101.03	2.61	N.S.